Methane producing and reducing microorganisms display a high resilience to drought in a Swedish hemi-boreal mire

J.D. White [1], D. Ahrén [2], L. Ström [1], J. Kelly [3], L. Klemedtsson [4], B. Keane [5], F-J. W. Parmentier [1,6]

[1] Department of Physical Geography and Ecosystem Science, Lund University, Lund, Sweden.

[2] National Bioinformatics Infrastructure Sweden (NBIS), Department of Biology, Lund University, Sweden.

[3] Centre for Environmental and Climate Science, Lund University, Lund, Sweden

[4] Department of Earth Sciences, University of Gothenburg, Gothenburg, Sweden

[5] Department of Animal and Plant Sciences, The University of Sheffield, Sheffield, United Kingdom

[6] Centre for Biogeochemistry in the Anthropocene, Department of Geosciences, University of Oslo, Norway

Corresponding author: Joel D. White (joel.white@nateko.lu.se)

Key Points:

- Taxonomic and functional gene composition significantly changed during the drought
- Methane fluxes significantly reduced during drought but not in all ecotypes
- Specialts genera respond to drought stronger than others

Abstract

An increased frequency of droughts due to anthropogenic climate change can lead to considerable stress for soil microorganisms and their functioning within northern peatlands. A better understanding of the diversity and abundance of methane producing and reducing taxa, and their functional genes, can help predict the functional potential of peatlands and how the microorganisms respond to disturbances such as drought. In order to address knowledge gaps in the understanding of how functional genetic diversity shifts under drought conditions, we investigated a hemi boreal mire in Southern Sweden. Environmental parameters, including soil and air temperature, precipitation and water table depth, as well as methane flux data were collected during the summer of 2017 under typical growing conditions, and in 2018 during a drought. In addition, the diversity and composition of genes encoding for methane metabolism were determined using the captured metagenomics technique. During drought we observed a substantial increase in air and soil temperature, reduced precipitation, and a lower water table depth. Taxonomic and functional gene composition significantly changed during the drought, while diversity indices, such as alpha and beta diversity, remained similar. These results indicate that methane producing and reducing microbial communities, and their functional genes, displayed a resilience to drought with specific genera having the ability to outcompete others under stress. Furthermore, our results show that although methane emissions are substantially reduced during drought, we can expect to see a shift towards more resilient methanogens and methanotrophs under future climate conditions.

Plain Language Summary

Droughts and heat waves are increasing due to climate change. This can lead to considerable stress on soil microorganisms in northern wetlands which emit strong greenhouse gases such as methane. A better understanding of these methane producing and consuming microorganisms can help us predict the how the community responds to droughts, and thus, how much green house gases will be emitted in the future contributing further to climate change.

1 Introduction

Anthropogenic climate change is one of the key issues of the twenty-first century, and it has the potential to severely impact natural peatlands through changes in temperature and precipitation (IPCC, 2021). While climate change models are forecasting increased precipitation at northern latitudes, these events are predicted to be more concentrated and less frequent in time with longer periods of dryer warm weather in between (IPCC, 2021). These events often result in a lowering of the water table depth which exposes methanogenic anaerobes to oxidative stress. This may decrease methane (CH_4) emissions to the atmosphere by reducing the habitable anoxic zone where methanogenic Archaea produce CH_4, but potentially also by increased activity and abundance of methanotrophs leading to a higher consumption of CH_4 (Keane et al., 2021, Rinne et al., 2020). These microbial communities inhabiting natural peatlands are vulnerable to disturbance under a warming climate, but potential structural shifts in microbial communities are currently difficult to predict, contributing to high uncertainties in current CH_4 budgets (Dean et al., 2018, Saunois et al., 2020).

Pristine peatlands function as long-term carbon sinks because plant productivity (CO_2 uptake) generally exceeds the slow rate of organic matter decomposition (CO_2 release) due to anaerobic

conditions. Although these anaerobic conditions lead to significant emissions of CH_4, over long-time scales, the carbon balance of peatlands is primarily determined by the CO_2 fluxes (Yu, 2012, Rinne et al., 2020). However, the greenhouse gas balance of a peatland can shift from a sink to a source after drought, when expressed in CO_2-equivalents, due to the higher global warming potential of CH_4 (Fenner and Freeman, 2011, Rinne et al., 2020).

Drought conditions, i.e. high air temperatures and reduced precipitation, result in a lower water table depth, aerating previously anoxic peat layers. This leads to increased heterotrophic respiration, and consequently a higher release of CO_2 to the atmosphere (Keane et al., 2021, Rinne et al., 2020). Concurrently, CH_4 emissions are reduced since oxygen (O_2) inhibits CH_4 production upon exposure to methanogen cells combined with increased methanotrophic CH_4 oxidization (Miller et al., 2019, Thauer et al., 2008). Due to these microbial controls, a deeper understanding of microbial structure and function, and the relationship to hydrological status, is required to improve projections of the role of peatland GHG emissions in the climate system.

Under anoxic conditions, inhibitory phenolic compounds are built up. These compounds prevent the activity of polyphenolic carbon degrading aerobes, which enable greater conversion of peat organic carbon into smaller substrates such as sugars, organic acids, H_2, and CO_2 that are more bioavailable for the anaerobic methanogens (Wilmoth et al., 2021, Fenner and Freeman, 2011). However, if O_2 is introduced through a drop in water table depth, phenol oxidase can remove phenolic inhibitors, enabling hydrolases to resume normal mineralization of organic matter that subsequently provide additional substrates for methanogenesis upon the return to anoxic conditions (Fenner and Freeman, 2011, Wilmoth et al., 2021).

The taxonomic structure and function of methanogens is diverse and closely linked to hydrology status and warming (Bräuer et al., 2020). CH_4 production occurs stepwise in cooperation between different microbial functional groups, where organic carbon bound to dead organic matter is converted into CH_4 via methanogenesis (Ferry, 1999, Dean et al., 2018). Methanogenesis is a process catalyzed by specialized functional groups that convert CO_2 with H_2, methanol, methylamines, methylsulfides, or acetate into CH_4 (Thauer et al., 2008). Anaerobic methanogenesis is carried out exclusively by members of the archaeal domain (Bräuer et al., 2020). Methanogens display high phylogenic diversity spanning three phyla (*Euryarchaeota*, *Halobacterota* and *Thermoplasmatota*) and are no longer considered strict *Euryarchaeota* members. In total, five orders and two candidate taxa are commonly discovered in peat: *Methanomicrobiales*, *Methanocellales* and *Methanosarcinales* of the phylum *Halobacterota*; *Methanobacteriales* of the phylum *Euryarchaeota*; *Methanomassiliicoccales* of the phylum *Thermoplasmatota*, and finally candidate family *Methanoflorentaceae* and candidate phylum *Bathyarchaeota* (Bräuer et al., 2020).

In contrast to methanogens, methanotrophs – of the phyla, *Proteobacteria*, *Verrucomicrobia*, and candidate phylum NC10 – can oxidize CH_4 before it is emitted to the atmosphere, acting as a natural bio-filter. Methanotrophs commonly inhabit the oxic-anoxic interfaces, where they oxidize between 10 to 90% of the CH_4 produced by methanogens (Hakobyan and Liesack, 2020, Wendlandt et al., 2010).

In this study, we focus on the drought that occurred during the summer of 2018 when Northwestern

Europe, including Sweden, experienced a heatwave (Rinne et al., 2020, Sjökvist et al., 2019, Vicente-Serrano et al., 2010). Lower precipitation and higher temperatures altered the hydrological status of Swedish peatlands, leading to a lower water table depth, increased peat temperatures, and altered biogeochemical processes – including changes to methanogenesis. Although, methanogenesis is one of the most important carbon degradation pathways in peatlands (Keane et al., 2021, Kelly et al., 2021), knowledge on the resilience of methanogenic archaea to droughts in terms of community abundance, diversity and structure is still poorly understood and requires further attention (Kim et al., 2008).

Here, we address the functional potential of methanogenic and methanotrophic microbes in response to drought. We hypothesise that (1) the proportion of methanogenic and methanotrophic community shifts in relative abundance towards higher methanotrophic abundances when exposed to drought conditions. In addition, we aim to (2) determine which vegetative ecotype holds the highest microbial diversity during the drought and (3), to identify whether the functional gene composition shifts in response to drought.

2 Materials and Methods

2.1 Site Description

This study focuses on Mycklemossen, a hemi-boreal mire dominated by bog-like vegetation, located in southern Sweden (58◦21'N, 12◦10'E). Mycklemossen is a sub-section of the Skogaryd Research Catchment and Swedish Infrastructure for Ecosystem Science network (https://www.fieldsites.se). Common to many hemi-boreal mires, the peatland consists of wet low areas dominated by *Sphagnum rubellum* and *Rhynchospora alba*, while the raised intermediate areas are a result of the tussock-building sedge *Eriophorum vaginatum*. Once the tussocks are established, the upper layers of the peat become drier and are no longer anoxic. This allows for the establishment of low shrubs such as *Calluna vulgaris.* The long-term (1990–2019) mean annual air temperature and total precipitation were 6.7°C and 1021 mm respectively, as measured by the closest national monitoring station (Vänersborg, 10 km to the east and at a 30 m lower elevation than Mycklemossen).

2.2 Experimental design

To determine the impact of the 2018 drought, we measured CH_4 fluxes, soil and air temperature, precipitation, water table depth, and collected peat samples for genetic analysis during 2017 and 2018. Measurements of CH_4 were made across a ~40 m long transect beginning at the tree line and extending into the mire. Plots were classified according to the dominant vegetation and are here represented as the *E. vaginatum* (n = 6), *C. vulgaris* (n = 6) and *R. alba* (n = 6) ecotypes. Replicate plots were identified at random and classified according to the dominant vegetation type. Peat samples for extraction of gDNA were removed from two different locations north and south of the boardwalk displayed in Figure 1. In 2017, 18 peat samples were collected from locations representing the *C. vulgaris* (n = 6), *E. vaginatum* (n = 8), and *R. alba* (n = 4) ecotypes south of the boardwalk (Figure 1). In 2018, 11 samples were collected from *C. vulgaris* (n = 2), *E. vaginatum* (n = 5), *R. alba* (n = 4) ecotypes north of the boardwalk (Figure 1). Peat sampling was conducted in two similar sampling locations north and south of the boardwalk and these were

separated by a distance of ~60m to avoid disturbance from previous sampling events (Figure 1). Both areas are similarly composed of hummocks and hollows and include equal representation of the pre-described ecotypes, which each exist within their own hydrological niche. The majority of the local peat deposits within the catchment extend down to 6 m depth (Wallin et al., 2015), with previous studies establishing no significant differences in surface or soil temperature between the hummocks and hollows (Kelly et al., 2021).

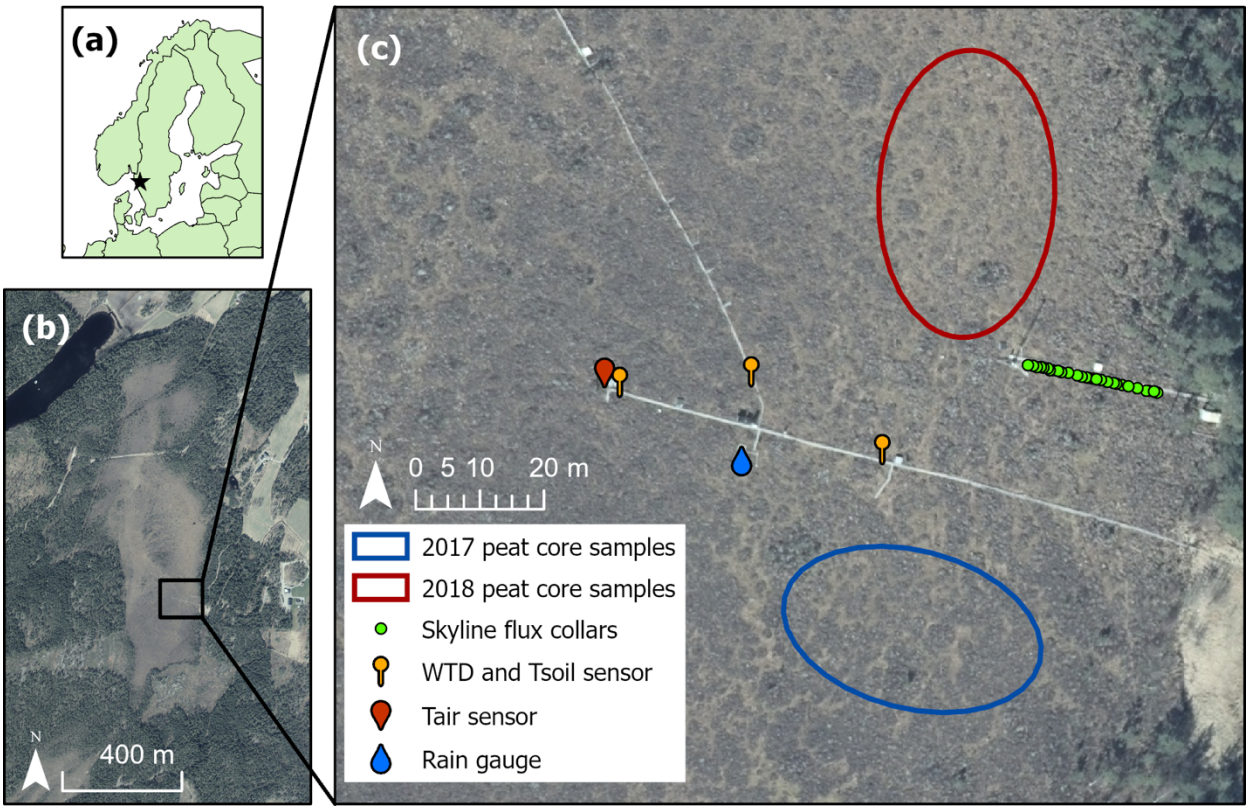

Figure 1: (a) Location of Mycklemossen (black star) within Sweden (b) aerial photo of Mycklemossen, black square shows the location of the sampling area and (c), map of peat core and ancillary measurement locations. Map data sources: © EuroGeographics and © Lantmäteriet.

2.3 Environmental variables

Meteorological variables were measured in both 2017 and 2018 with which we characterized the severity of the drought at Mycklemossen. Air temperature was measured with an HC2S3 sensor (Campbell Scientific, Logan, UT, USA) at 2 m above the peatland surface in a ventilated, radiation protected housing. Precipitation was measured with a tipping bucket rain gauge (SBS500H, Campbell Scientific, United Kingdom). Water table depth (CS450, Campbell Scientific, UT United States) was measured at three different locations that represented the *C. vulgaris*, *E. vaginatum* and *R. alba* ecotypes. The locations for soil and air temperature, precipitation and water table depth sensors are shown in Figure 1. All environmental variables were measured at 1 Hz and recorded on a CR1000 data logger (Campbell Scientific, UT United States). Air temperature and water table depth values were averaged to represent daily means, while precipitation was summed to represent total daily values.

2.4 CH_4 flux measurements

Surface GHG fluxes were measured using the SkyLine2D system. The SkyLine2D is an automated chamber system designed and built at the University of York to measure greenhouse gas exchange. For a full description of the SkyLine2D system, we refer to Keane et al. (2018). In short, the flux chamber comprised of a translucent Perplex cylindrical chamber (inner diameter 20 cm, height 40 cm), which was suspended from a motorized trolley and programmed to traverse ca. 2 m above the transect. The system was preset to visit the pre-selected plots along the transect, where the chamber was lowered onto pre-installed collars for a measurement period of 4 minutes. Following the 4-minute measurement period, the system raised the chamber and moved to the next plot. The time taken to complete a full cycle was approximately 2.5 h, which allowed each chamber to be measured ca. 10 times per day. The headspace gas from within the sealed chamber was circulated through a Los Gatos cavity ring-down laser (CRD, LGR U-GGA-91, Los Gatos Research, CA United States) to measure the change in concentration of CH_4. Fluxes were calculated as the increase in headspace concentration over time, determined by linear regression, and adjusted for temperature and area of the chamber.

2.5 Captured metagenomics

2.5.1 DNA extraction

Peat material was collected using a 1.5m long box corer from different locations within the mire that best represented the dominant ecotypes (Figure 1). Small samples of peat (~30 grams) were collected from the oxic-anoxic interface at ~5cm and within the anoxic zone, at ~30cm. Once separated from the cores, the peat material was immediately snap frozen using liquid nitrogen and stored in a -20°C freezer. Before DNA extraction was performed, samples were thawed in a refrigerator at 4°C. After thawing, gDNA was extracted from peat samples following the DNeasy® PowerSoil® Kit (Qiagen, Hilden, Germany) and carried out according to the manufacturers protocol, including the recommended 0.25g of input material. Following the DNA extraction, samples were tested for quality (absorbance ratio 260/280) and concentration on a NanoDrop lite (NanoDrop Technologies, Wilington NC, USA) and Invitrogen Qubit 4 fluorometer (Thermo Fisher Scientific, Waltham MA, USA) respectively.

2.5.2 SeqCap EZ probe generation

The metagenomic DNA extracted from the peat was processed to enrich for sequences of interest via the "captured metagenomics" method using oligonucleotide probes following White et al. (2022) and Manoharan et al. (2015). In short, genes that encode enzymes related to methane production and consumption were identified from the Kyoto Encyclopedia of Genes and Genomes database (KEGG) (Kanehisa et al., 2015). In total, 548,104 genes coding for methane metabolism were downloaded via a custom R script (https://github.com/dagahren/metagenomic-project) and compiled into a local database, subsequently called the CH_4 database. The nucleotide coding sequences of the CH_4 database were used to design custom hybridisation-based probes for sequence capture according to Kushwaha et al. (2015). In total, 193,386 individual probes were generated after clustering, with a melting temperature of 55°C and probe length 40mer, suitable for use with the NimbleGen SeqCap EZ protocol (Roche NimbleGen Inc., Madison, USA).

2.5.3 Library generation, probe hybridisation and sequencing

Depending on the concentration of the extracted DNA in a total volume of 100µl low TE, either 150ng or 1µg of gDNA was sheared using a Bioruptor Pico in 0.65ml Bioruptor tubes for 13 cycles – 30s on, 30s off (Diagenode SA, Seraing, Belgium). The fragmented DNA was purified using 1.8× AMPure XP beads (Beckman Coulter) and used as input material for preparation of pre-capture libraries. Libraries were constructed according to the Nimblegen SeqCap EZ HyperCap Workflow User's Guide (Version 1.0, June 2016) with the following modifications: (1) for the adapter ligation step, 5µl of 15µM KAPA unique dual index mixed adapters were used instead of single index adapters, (2) for the pre-capture PCR, 7 cycles were used for libraries with a genomic DNA input of 150ng, and 5 cycles where the input was 1µg.

Libraries were multiplexed in pools of 15 in equimolar amounts based on the concentrations and sizes. 1µg of each pool was transferred to a test tube and hybridised to the custom probes according to the NimbleGen SeqCap EZ SR User's Guide (Version 4.3, October 2014). The capture tubes were incubated in a thermal cycler set at 47 ºC, heated lid set to 57 ºC for 69 hours. The quantity and quality of the final pool was assessed by Qubit and Bioanalyzer and subsequently by qPCR using the Illumina Library Quantification Kit from Kapa on a Roche Light Cycler (LC480II, Basel, Switzerland).

The captured libraries were sequenced on an Illumina HiSeq4000 platform using sequencing by synthesis technology to generate 2 x 150 base paired end reads. The analysis was carried out at the Centre for Genomic Research, University of Liverpool, United Kingdom.

2.6 Data processing and statistics

2.6.1 Environmental variables

All environmental data, including soil and air temperatures, precipitation and water table depths were measured from the 1st of May to the 30th of September, which we refer to as the growing season. In addition, we tested for differences in the mean values of air temperature, soil temperature and water table depth, according to the defined ecotypes, between 2017 and 2018.

2.6.2 CH_4 flux

CH_4 flux data was quality controlled by discarding measurements with a R^2 value $\leq$ 0.9. Measurements passing this threshold were then assessed using the output statistics from the regression calculation, where regressions with a p value $\leq$ 0.05 were accepted, while those that did not were treated as zero flux. To allow for the temporal and repeated measures data, differences in CH_4 fluxes between years and ecotypes were tested using linear mixed effects models via the lme4 package v1.1-27.1 (Bates et al., 2015). Differences were calculated using estimated marginal means in combination with a Tukey pairwise post-hoc tests on significant effects.

2.6.3 Sequence annotation

Raw sequencing files were trimmed for the presence of Illumina adapter sequences using the software package Cutadapt v1.2.1 (Martin, 2011). The reads were further trimmed

using Sickle v1.2 with a minimum window quality score of 20 (Joshi, 2011). Following trimming, reads shorter than 20bp were discarded. The sequence reads from each of these captured data sets were processed through MG-RAST, an online metagenomics annotation program (Meyer et al., 2008). Default parameters were used for quality filtering of low quality reads and removal of sequence duplicates. The taxonomic and functional annotations from MG-RAST were annotated using the RefSeq (O'Leary et al., 2016) and KEGG (KO) (Kanehisa et al., 2015) databases. Following the MG-RAST pipeline, sequences were further filtered for both taxonomic and functional gene annotations using the KEGG methane metabolism filter (ko:00680). The filter includes both taxonomic and functional genes related to methane metabolism and excludes remaining off target sequences. Sequence data and functional annotations are freely available through MG-RAST with the accession ID mgp91145. These filtered sequences were then exported to R for further analysis.

2.6.3 Taxonomic diversity and functional genes

Diversity indices were calculated via the phyloseq package v1.3.0 (McMurdie and Holmes, 2013) where taxonomic abundances below 10 reads were removed. Due to the small sample sizes and uneven distribution of replicates, a PERMANOVA was used with 999 permutations (Anderson, 2001). First, we normalized taxonomic and functional gene relative abundance via a double square root transformation to allow for highly abundant genes. Following transformation, we calculated ordination using Bray-Curtis distances and finally, a Wilkson pairwise post-hoc test was used to identify significant differences between ecotypes and years with the vegan package v2.5 (Oksanen et al., 2019). All analyses were completed in the R statistics package v 3.6.1 (R Core Team, 2018) and visualized using the ggplot2 package v 3.3.2 (Villanueva and Chen, 2019).

3.0 Results

3.1 Environmental variables

In 2018, Mycklemossen mire experienced a maximum air temperature of 33°C that was reached on the 31st of July 2018 (Figure 2A). Daily mean air temperature during May-September reached a maximum of 24.8°C (SD ± 3.95) in 2018, a 5.6°C increase in comparison to 2017. On average, all daily mean soil temperatures during the growing season were higher in 2018 when compared to 2017. The high air temperature was also reflected in the soil temperature, where the maximum daily values in August 2018 were 3.4°C higher at 6cm depth and 1.3°C higher at 30cm depth in the *C. vulgaris* ecotype compared to 2017 values (Figure 3, A and B). The *E. vaginatum* ecotype followed the same pattern with 2°C higher at 6cm depth and 1.5°C higher at 30cm depth (Figure 3, C and D). The final ecotype, *R. alba,* had a slightly lower deviation with 1.4°C higher at 6cm depth and 1.2°C higher at 30cm depth (Figure 3, E and F).

Daily summed precipitation values in 2018 were below average during the growing season from May to October (Figure 2B), with predominantly dry conditions in July 2018 when only 10.2 mm of rain was recorded, compared to the long-term average of 80 mm. Significantly lower rainfall was observed in 2018 during the whole growing season when compared to 2017 values ($p \leq 0.04$) (Figure 3). This decrease in precipitation resulted in a lower water table depth across the whole peatland (Figure 4). Significantly lower WTD's were observed in both *E. vaginatum* ($p \leq 0.02$) and *R. alba* ($p \leq 0.02$), resulting in a lower water table depth up to 4 cm and 9 cm in 2018 (Figure

4B*)*. In the *C. vulgaris* ecotype, the water table dropped by as much as 7 cm in 2018 when compared to 2017.

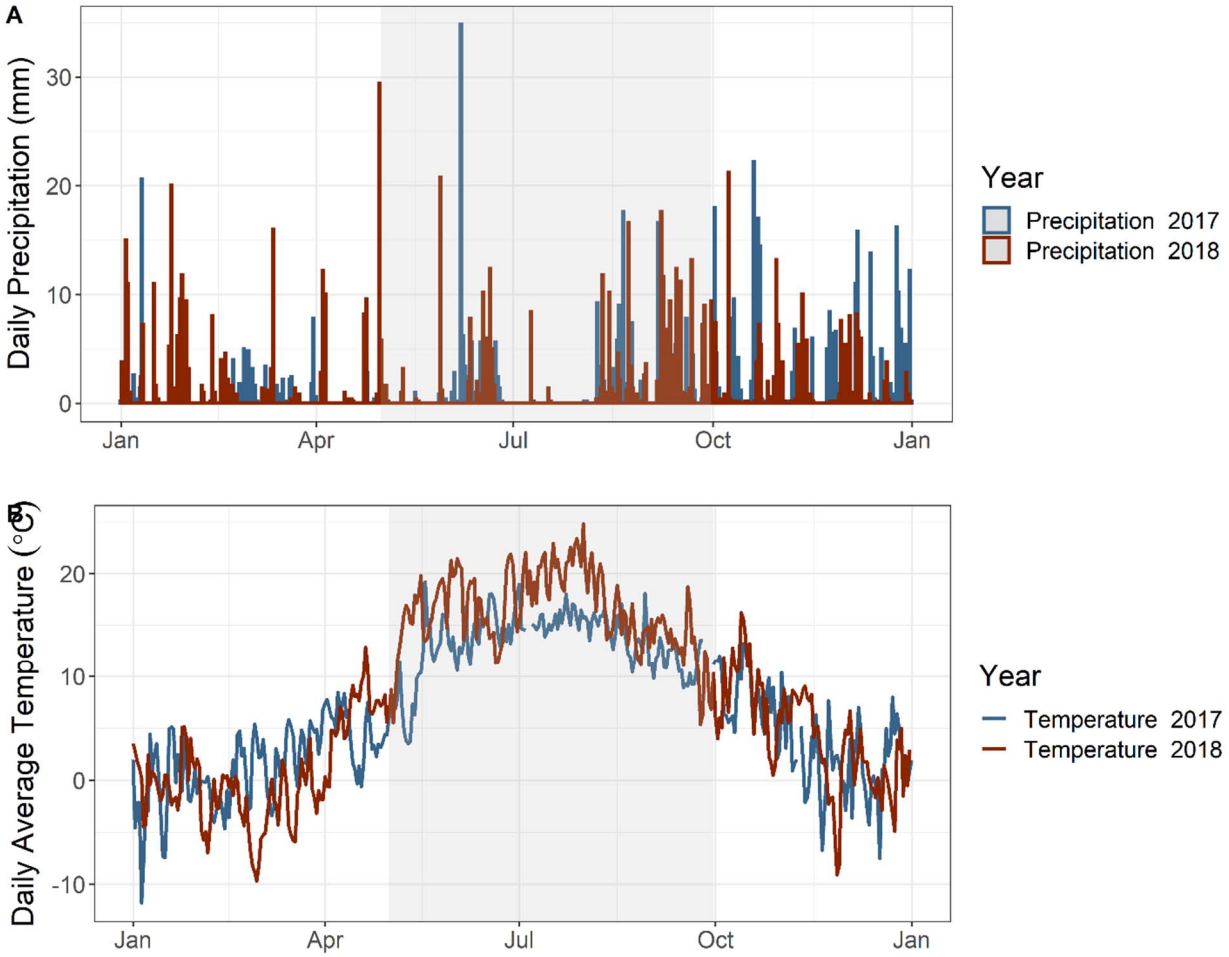

Figure 2: A) Daily mean temperature measured in °C and B) Daily summed precipitation measured in millimeters at Mycklemossen mire. 2017 is shown in blue and 2018 in red. The shaded area indicates the growing season from May 1st to September 30th.

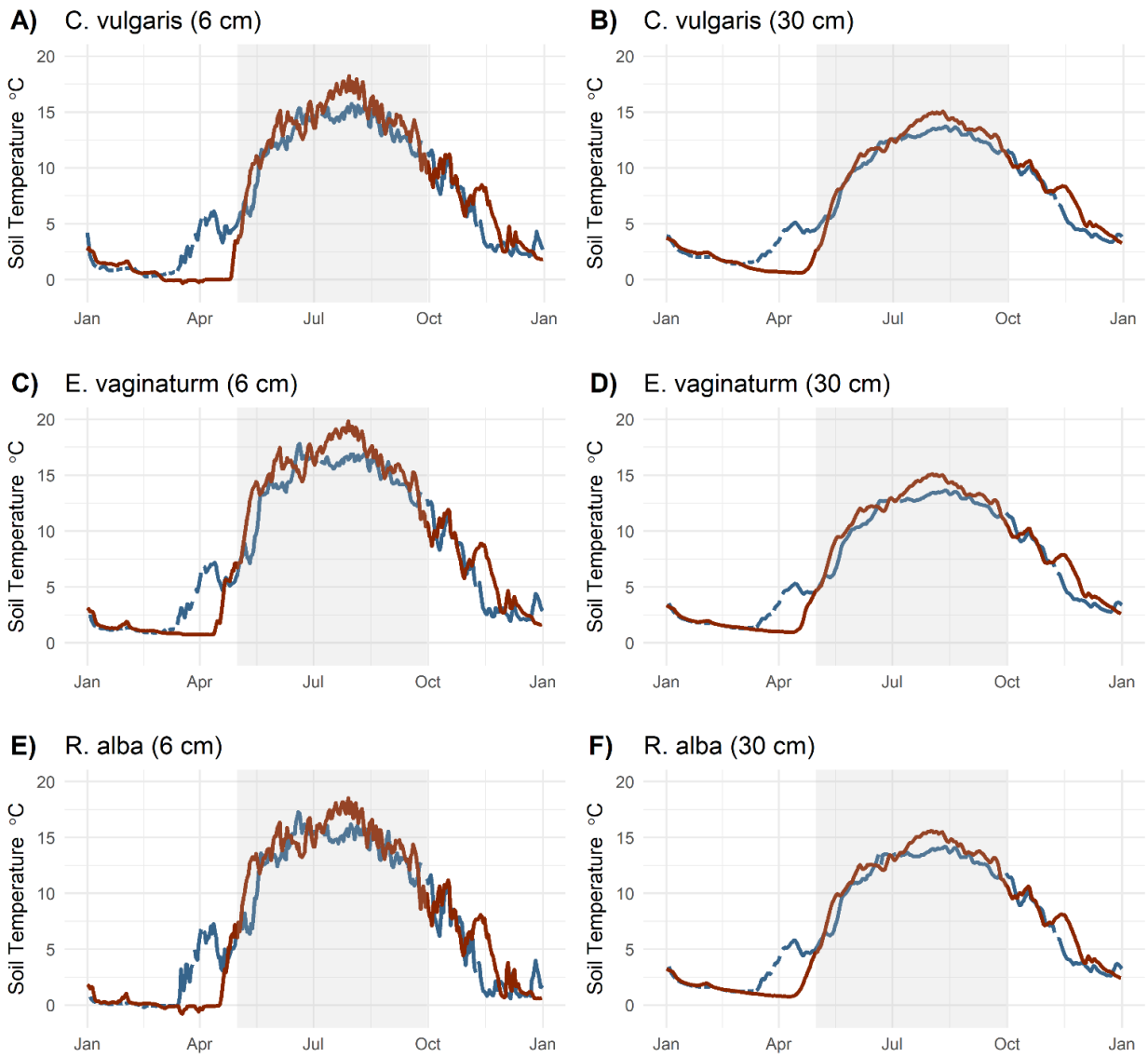

Figure 3: Daily mean soil temperature measured at 6 cm and 30 cm below the peat surface. Blue lines indicate 2017 values while red lines indicate 2018 values. The shaded area indicates the growing season from May 1st to September 30th.

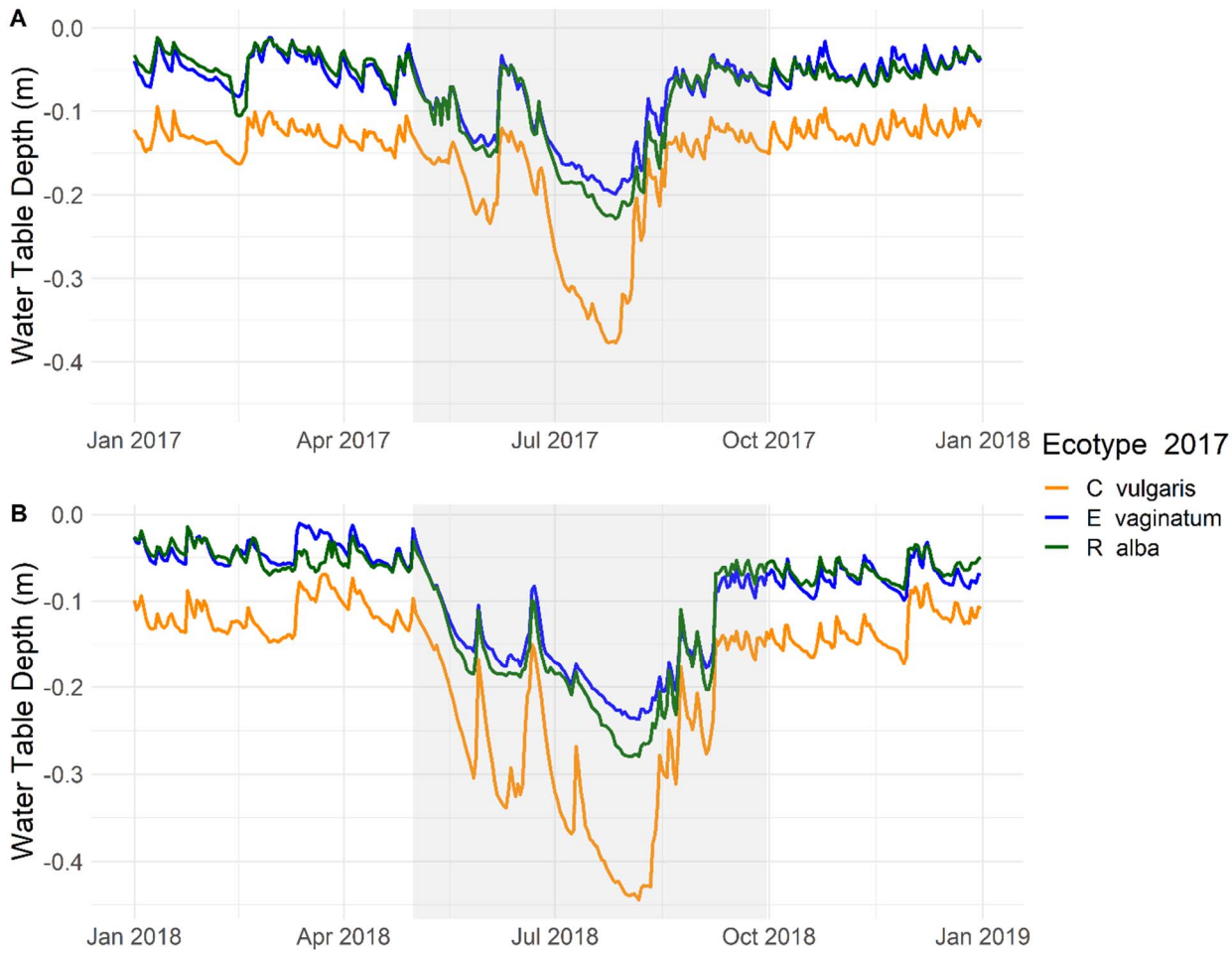

Figure 4: Water table depth in meters below the surface for *C. vulgaris*, *E. vaginatum* and *R. alba* ecotypes from automated sensors at the site during 2017 (A) and 2018 (B). The shaded area indicates the growing season from May 1st and September 30th.

3.2 Methane fluxes

The highest daily mean CH_4 fluxes (33.3 CH_4 nmol m^{-2} s^{-1}) were observed during the growing season in 2017, significantly higher than in 2018 (25.7 CH_4 nmol m^{-2} s^{-1}) ($p \leq 0.001$). The ecotype that yielded the highest mean CH_4 flux was *R. alba* in 2017 with a mean flux of 48.1 CH_4 nmol m^{-2} s^{-1} (SD ± 3.11) followed by *E. vaginatum* (34.1 SD ± 6.36 CH_4 nmol m^{-2} s^{-1}) and *C. vulgaris* (17.8 SD ± 2.58 CH_4 nmol m^{-2} s^{-1}). During the drought in 2018, fluxes in the *R. alba* ecotype significantly reduced by 29% ($p \leq 0.0001$), and by 27% ($p \leq 0.04$) in the *C. vulgaris* ecotype, while the smallest reduction was observed in *E. vaginatum* (10%) ($p \geq 0.05$).

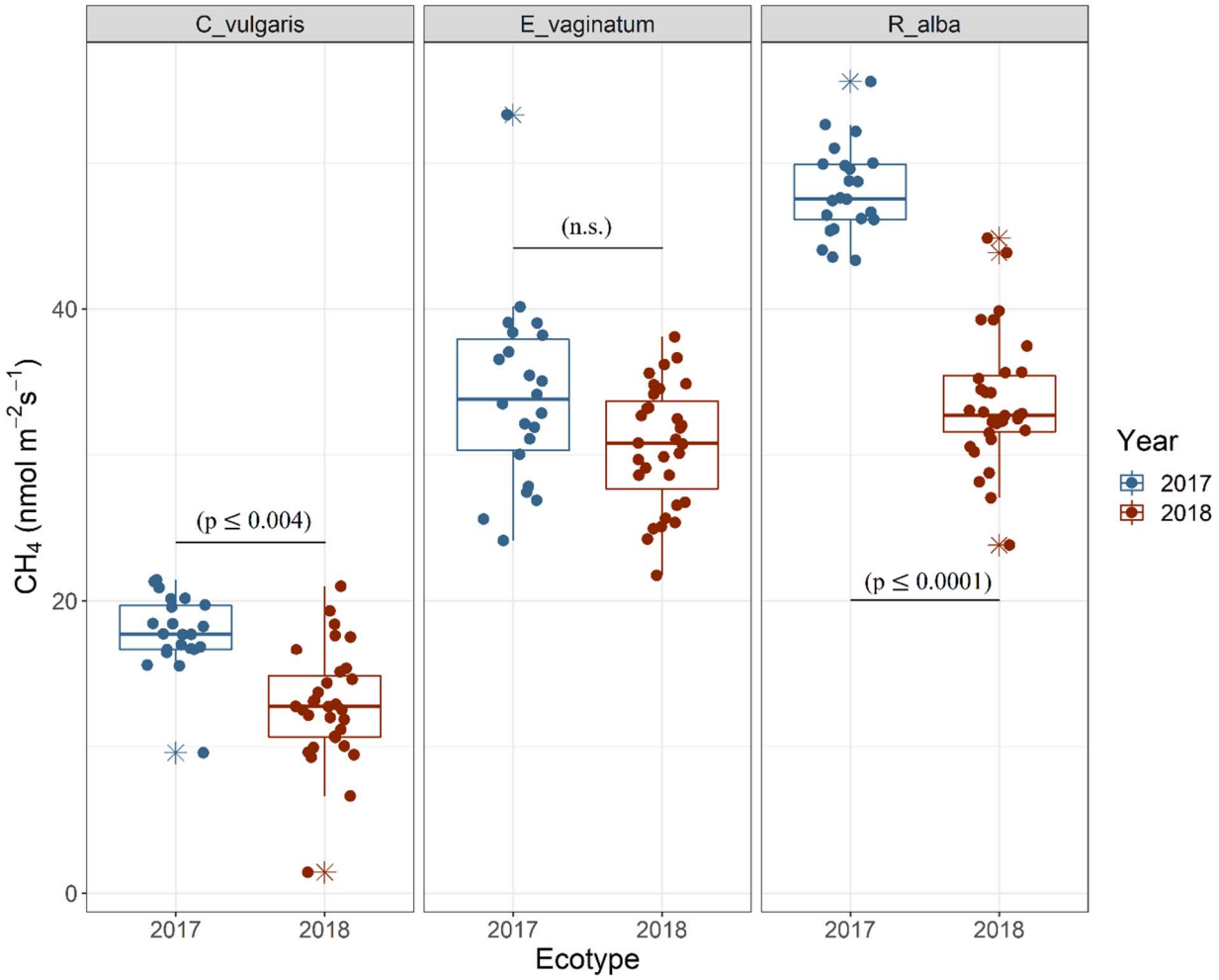

Figure 5: Boxplots of daily mean CH_4 flux measured during the growing season (May to October) in 2017 (blue) and 2018 (red) at Mycklemossen mire. The boxes show quartiles and the median, the whiskers denote data within 1.5 times of the interquartile range. Colored stars denote outliers while significant differences using linear mixed effects models are labelled with the p value and "n.s." indicates a non-significant result.

3.3 Taxonomy

3.3.1 Proportions of methanogens to methanotrophs between years

Large significant variations in the abundances of methanogens and methanotrophs were observed between drought and non-drought years, with 36% of the variation explained by the year (R^2 = 0.36, $p \leq 0.003$) (Figure 6). Clear clusters can be observed in Figure 6 with only a small overlap in samples. The average proportion of methanogens to methanotrophs during 2017 was 59% and 41% respectively. In 2018, however, the proportion of methanogens decreased by 8%, while the proportion of methanotrophs increased to 49%. The genus which contributed the most to dissimilarity according to the SIMPER analysis – that calculates the contribution of each species (%) to the dissimilarity between each group – was *Methylocella,* with an 0.12 average contribution to the overall dissimilarity (Table 1). The average abundance for *Methylocella* significantly increased by 219% during the drought in 2018 when compared to 2017 ($p \leq 0.001$). Interestingly,

the average abundance of all methanogens and methanotrophs increased during the drought, with *Methanoregula* contributing the highest to dissimilarity, followed by *Methanosarcina*. In addition, all detected methanotrophs significantly increased, including the type I, II and *Verrucomicrobia* when tested between years ($p \leq 0.005$).

Table 1: Results of taxonomic contribution of each species (%) to the dissimilarity between each group (SIMPER analysis) between 2017 and 2018. Taxa are ranked according to their average contribution to dissimilarity between years. Average abundances, percentage of cumulative contribution and Permutation *p*-value (Probability of getting a larger or equal average contribution in random permutation of the group factor) are also included. A cut-off at a cumulative dissimilarity of 70% was applied (2017 n = 17: 2018 n = 10).

Genus	Average contribution to dissimilarity	SD	Avg. 2017	Avg. 2018	Percentage contribution	p-value
Methylocella	0.12	0.089	2539	8108	20%	0.001
Methanoregula	0.09	0.085	4267	5968	36%	1
Methylosinus	0.08	0.050	2386	5602	49%	0.031
Methanosarcina	0.05	0.032	1529	4142	58%	0.006
Methylococcus	0.03	0.022	814	2495	64%	0.001
Methylacidiphilum	0.03	0.020	568	1935	69%	0.001

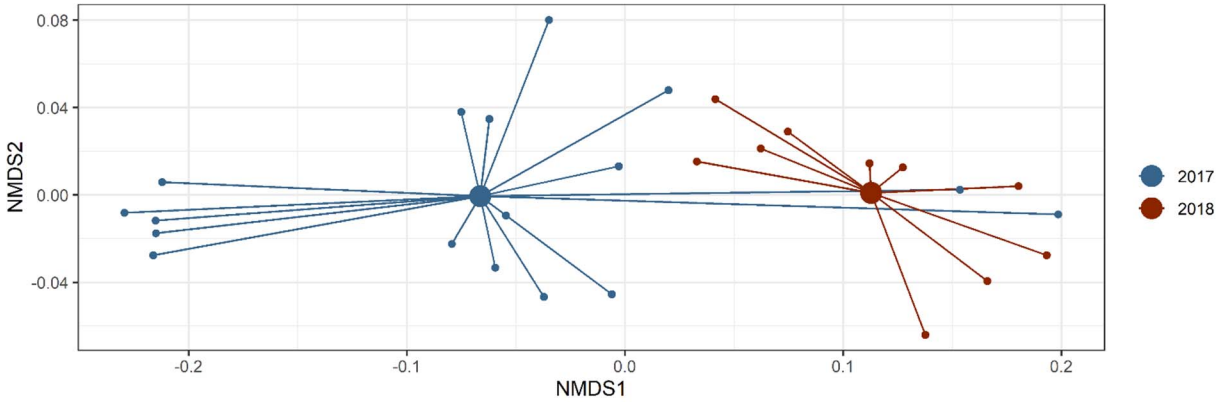

Figure 6: Non-metric Multidimensional Scaling (NMDS) of taxonomic abundances using Bray-Curtis distances. Small dots indicate individual samples while the largest dots indicate the mean of all samples. Samples were analyzed at genus level and colored by year 2017 (n = 17) and 2018 (n = 10).

3.3.2 Ecotype comparison

A large dissimilarity in the relative abundance of taxa was observed when comparing ecotypes between each year. This variation in taxonomic abundance resulted in a significant correlation where 58% of the variation in taxonomic abundance could be explained by ecotype ($R2 = 0.58$, $p \leq 0.002$). The Wilks pairwise test indicated that significant dissimilarity occurred for E. vaginatum between 2017 and 2018 ($p \leq 0.03$), but the same dissimilarity was not observed for R. alba and C. vulgaris ($p \geq 0.05$).

When comparing the relative abundance of methanogens and methanotrophs between *E. vaginatum*, *R. alba* and *C. vulgaris*, six genera were the most common within the top 70% of cumulative sums, irrespective of ecotype: *Methanoregula*, *Methylocella*, *Methylosinus*, *Methanosarcina*, *Methylococcus* and *Methylacidiphilum* (Supplementary table 1, 2 and 3). *Methanocaldococcus and Methanosphaerula* were within the top 70% of cumulative sums for the *R. alba* ecotype (Supplementary table 2), but not *E. vaginatum* (Supplementary table 1) or *C. vulgaris* (Supplementary table 3).

When comparing *R. alba* and *C. vulgaris,* we observe that the hydrogenotrophic *Methanoregula* contributed the most to dissimilarity (Supplementary Table 2 and 3). Although type II *Alphaproteobacteria genera, Methylocella* and *Methylosinus* were the second and third most important between ecotypes, the order of dissimilarity of *Methylocella* and *Methylosinus* changed according to ecotype. Within the *E. vaginatum* comparison, the dominant *Methanoregula* was surpassed by *Methanosarcina,* with an average dissimilarity of 0.07, when compared to the remaining ecotypes.

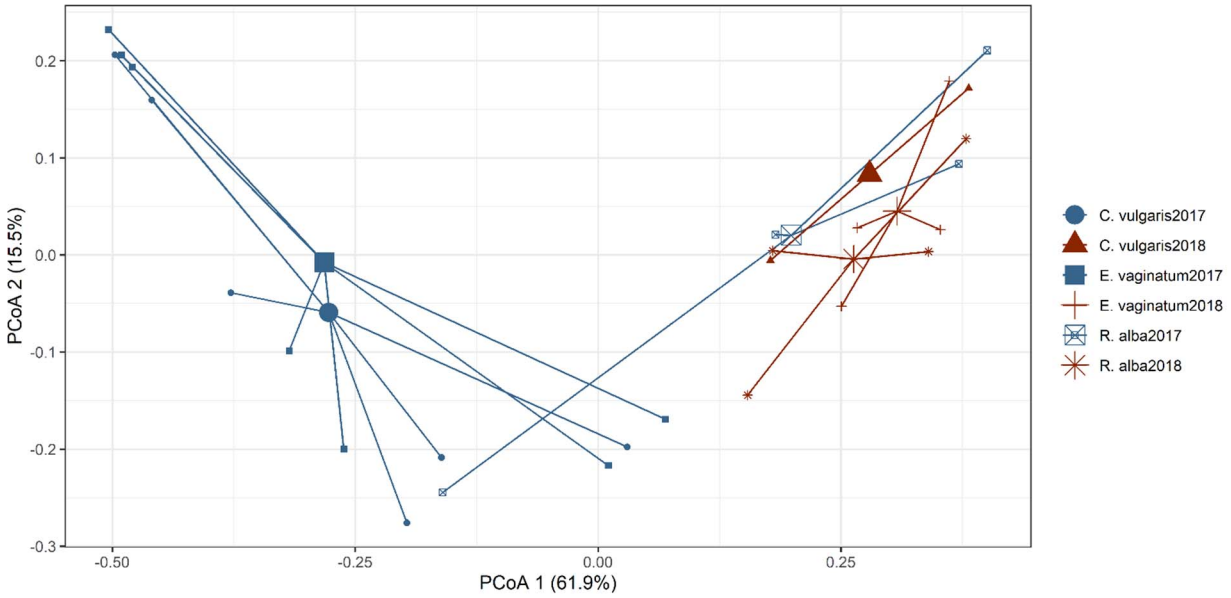

Figure 7: Principal Coordinates Analysis (PCoA) of taxonomic abundances using Bray-Curtis distances. Small symbols indicate individual samples while the largest symbols indicate the mean of all samples. Samples were analyzed at genus level and colored by ecotype and sampling year

(*C. vulgaris* 2017 (n = 6) 2018 (n = 2), *E. vaginatum* 2017 (n = 7) 2018 (n = 4), *R. alba* 2017 (n = 4) 2018 (n = 4).

3.5 Functional gene composition

The functional genes showed a clear separation between 2017 and 2018, with only a small overlap between clusters (Figure 8). The largest variation of functional genes occurred in 2017, with smaller variation observed in 2018. Significant differences were observed between the abundance of functional genes when tested via PERMANOVA between 2017 and 2018 ($p \leq 0.036$). In addition, the PERMANOVA revealed that 12% of the variance in abundances can be explained by the year ($R^2 = 0.12$, $p \leq 0.036$).

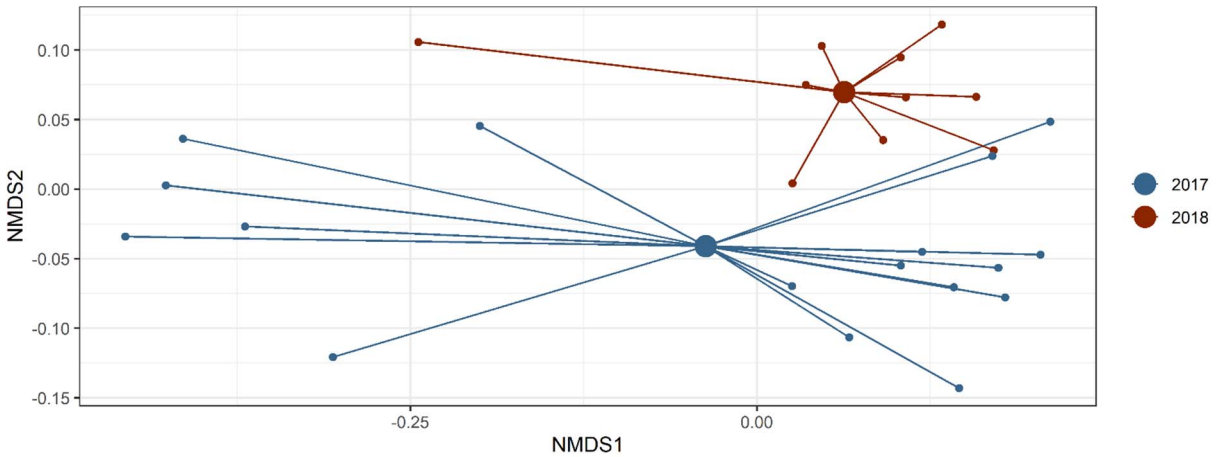

Figure 8: Nonmetric Multidimensional Scaling (NMDS) of functional genes using Bray-Curtis distances. Small dots indicate individual samples while the largest dots indicate the mean of all samples. Samples were analyzed at KO level 4 and colored by year 2017 (n = 17) and 2018 (n = 10).

In total, 106 functional genes related to CH_4 metabolism were captured, with 20 contributing to the top 70% cumulative sum of dissimilarity between CH_4 functional genes (Supplementary Table 4). Within the top 70% cumulative contributions, 12 out of the 20 captured genes saw an increase in average abundance in 2018. The gene contributing most to the dissimilarity was heterodisulfide reductase subunit A (*hdrA*). The *hdrA* gene held an average abundance of 627 in 2017, resulting in an 86% increase in 2018 ($p \geq 0.05$). Genes including *cutL*, *hdr*, *fdhA, coxS, frmB, mvhA, metF* and *cutM* were all significantly more abundant in 2018 when compared to 2017 values ($p \leq 0.05$). Genes that did not increase during 2018 included *frhA, mcrA, frhG, hdrB, fwdB, mtd, mtrE and mtrH*.

4.0 Discussion

In this study, we observed the effect of drought on the functional potential of CH_4 producing and reducing microorganisms. In general, methanogens and methanotrophs displayed a high resilience

to drought conditions, with shifts in proportion towards more methanotrophs. In addition, the relative abundance of methanogens and methanotrophs increased – with large increases observed within genera with expanded genomic features that enable better tolerance towards oxidative environments.

4.1 Structural shifts in response to drought

CH_4 emissions from peatlands have been largely attributed to the metabolism of methanogens, balanced by oxidation via methanotrophs (Dean et al., 2018). Here, we hypothesised that the proportion of methanogenic community shifts towards more methanotrophic relative abundances when exposed to drought conditions. This hypothesis was confirmed when we observed an increase of 8% in the relative abundance of methanotrophs during drought. The proportion of methanogens reduced by 8% in favor of methanotrophs under drought conditions. This shift was also reflected in the CH_4 flux, where both *C. vulgaris* and *R. alba* ecotypes had significantly lower fluxes during the drought. However, in the *E. vaginatum* ecotype, a significant reduction was not observed, despite showing the same trend as the other ecotypes. We hypothesise that the drop in water table depth led to increased O_2 availability, increased phenol oxidase activity and higher peat temperatures. This shift in habitable zone within the peat profile provided a new ecological niche for methanotrophs and other bacteria to expand into, which were previously un-inhabitable for methanotrophs due to the anoxic conditions and high concentration of phenolic compounds. This result is in agreement with findings from Amodeo et al. (2018), where the authors reported that the optimum growth for methanotrophs is between 20°C and 25°C combined with a 1:1 ratio of CH_4:O_2. Therefore, the increased peat temperature, newly habitable oxic zone and CH_4 originating from deeper anoxic layers led to increased abundances of methanotroph communities during the drought.

The three main methanotrophs driving the increased proportion under the drought were type II: *Methylocella*, *Methylosinus* and type I: *Methylococcus*. Type II genus *Methylocella* and *Methylosinus* contributed the highest to the total microbial sum, which was also observed in previous studies (Ho et al., 2011). Ho et al. (2011) observed the same pattern of rapid initial growth of type II methanotrophs in severely disturbed microcosms from rice paddies, whereas growth of type I methanotrophs were stunted. Although type I methanotrophs were not stunted in our results (i.e., *Methylococcus*), type II methanotrophs increased more in proportion when compared to type I, indicating that type II methanotrophs are highly adaptive to drought conditions and are not limited by their main substrates CH_4 and O_2 and other nutrients, but rather, the amount of habitable zone within the peat column.

Interestingly, the relative abundance of both methanogens and methanotrophs increase during drought. Several studies concluded that methanogenesis is suppressed upon exposure to O_2 (Ma et al., 2012, Yuan et al., 2009), while we observed a reduction in CH_4 flux but not a total cessation of CH_4 emissions. The same was observed by Rinne et al. (2020) and similar results have been observed in flooded paddies, lake sediments and bromeliad tanks where members belonging to *Methanocellaceae* and *Methanosarcinaceae* increase in relative abundance following desiccation (Brandt et al., 2015, Conrad et al., 2014). One explanation to the increase in relative abundance can be explained by methanogens including *Methanoregula*, *Methanosarcina* and *Methanosphaerula* that possess expanded genomic features that enable better adaptation to

oxidative environments (Lyu and Lu, 2018). In this study, the abundance of the dominant methanogen, the hydrogenotrophic *Methanoregula*, remained unchanged during both drought and non-drought conditions, neither decreasing nor increasing significantly. However, the most metabolically versatile of the methanogens, *Methanosarcina,* increased significantly under drought conditions within the ecotype *E. vaginatum*, presumably due to the presence of oxygen-detoxifying enzymes such as catalase, superoxide dismutase, and superoxide reductase that give this methanogen a particular eco-physiological advantage that allows for growth during desiccation (Angel et al., 2011, Erkel et al., 2006, Conrad et al., 2014). Therefore, the physiological characteristics of the community indicate that both hydrogenotrophic and acetoclastic methanogens, especially facultative methanogen members belonging to the class *Methanosarcinales,* that are more resilient to drought conditions and O_2 than other genera observed here.

Methanogenesis and microbial growth are temperature dependent processes (van Hulzen et al., 1999). Although methanogenesis can be inhibited when exposed to O_2, our flux measurements show that not all methanogenesis stopped. It is possible that, following the drop in water table, not all water evaporated, resulting in peat macropores acting as anoxic microbial refuges. It is also possible that microscale anoxic sites are formed within soil aggregates, which provide an ecological refuges for the survival of methanogens exposed to O_2 stress (Yuan et al., 2009). These ecological refuges still hold the necessary environmental conditions for methanogenesis to occur, but with an increased temperature that can increase metabolic activity.

Incubation studies by van Hulzen et al. (1999) found that alternative electron acceptor reduction increases with a rise in temperature, indicating that available electron acceptors will be reduced sooner – resulting in increased methanogen growth. When all alternative electron acceptors are consumed, the population size of the methanogens is the limiting factor in CH_4 production. Therefore, increased soil temperature coupled with the eco-physical advantage demonstrated by multiple functional groups may explain the increased relative abundance of methanogens during the drought, which is consistent with other studies (Brandt et al., 2015, Conrad et al., 2014).

During drought and the lowering of the water table, the relative abundance of aerobic methanotrophs increased significantly. Previously uninhabitable anoxic environments within the peat column became aerobic, allowing a competitive edge for genera such as *Methylocella* and *Methylosinus,* which are strict aerobes. Previous studies have reported increased methanotroph abundance associated with higher magnitudes of CH_4 flux (van Hulzen et al., 1999, White et al., 2022), however the same results are not observed here, indicating that the reduction in CH_4 flux is caused by an increase in methanotrophy. *Methylocella,* a facultative methanotroph, was the dominant methanotroph in all ecotypes. This trend can be explained by its capability of growing on CH_4 as well as on multicarbon substrates (Dedysh and Dunfield, 2011). This means that under stressful conditions such as drought, *Methylocella* can metabolize via multiple alternative metabolic pathways, yielding a competitive advantage over other obligate methanotrophs. These results are further confirmed by Ho et al. (2015) and Ma et al. (2012), where they showed that the recovery of type I methanotrophs needed more time between drying events. Therefore, during a drought we expect type II methanotrophs to dominate. Our results indicate that methanotrophs are highly resilient to droughts, but their resilience may still reach a 'critical point' where activity is no longer recovered if droughts persist on longer time scales and increase in frequency.

4.2 Taxonomic diversity between ecotypes

During the drought, the overall diversity of methanogens and methanotrophs did not change. To identify whether the overall diversity shifts following drought, and which peatland ecotypes holds the highest resilience, we assessed α-diversity and between-ecotype β-diversity. We observed small non-significant variation in the means of α-diversity between drought and control years. These findings are in line with results from Kim et al. (2017), where there were no differences in the diversity and composition of the microbial communities between control and a 4 week drought. In contrast, Zhong et al. (2017) showed significant difference in observed species and Shannon α-diversity of prokaryotic microbiota following water table draw down. However, these results were based on a 46-year time interval where the original peatland was drained for livestock grazing. These results indicate the need to research the effects of repetitive and long-term disturbance from drought in the future. Therefore, we conclude that the resilience of methanogens and methanotrophs to the effects of drought is high in the short term, but more research is needed on the effects on community structure and function during sustained droughts.

4.3 Effect of ecotype on CH_4 fluxes

During the drought, significantly lower CH_4 fluxes were observed in *C. vulgaris* and *R. alba* ecotypes, but not in *E. vaginatum*, although a similar trend was detected. We believe that the presence of aerenchyma tissue within the sedge *E. vaginatum* tillers, plus the ability for the sedge species to access anoxic layers through deep roots, allowed access to CH_4 produced in deeper anoxic layers. This physiological trait facilitates the transport of CH_4 produced in deep anoxic peat layers directly to the atmosphere, by-passing aerobic upper layers where methanotrophy can oxidise CH_4. Our results are consistent with previous studies conducted in peatlands where vegetative cover is directly related to the magnitude of CH_4 flux (Keane et al., 2021, Korrensalo et al., 2018).

The ecotype with the largest reduction in CH_4 emissions during the 2018 drought was *R. alba*. This ecotype is usually dominated by high water table depths and sphagnum mosses, indicative of conditions favoring CH_4 production. Interestingly, previous studies conducted across the globe have identified moss-associated methane oxidizers inhabiting *Sphagnum* (Kip et al., 2010), and revealed that moss-associated methane oxidizers can exceed methanogenic activity in terrestrial sites by up to two orders of magnitude (Liebner et al., 2011), but this relationship was not observed in our results. One possible explanation is the presence of *R. alba*, a sedge species with aerenchyma tissue similar to *E. vaginatum*. However, the rooting length of *R. alba* is substantially more shallow than *E. vaginatum,* resulting in limited access to deep anoxic layers. Thus, we do not observe the same by-passing of aerobic upper layers where methanotrophs can oxidize CH_4, therefore reducing net CH_4 emissions.

Finally, the *C. vulgaris* ecotype had the lowest CH_4 emissions in both 2017 and 2018, consistent with previous studies (Keane et al., 2021). *C. vulgaris* dominated the drier portion of the bog, where it is expected to see a combination of low methanogenesis and high methanotrophy, due to the aerobic conditions and lack of plant mediated CH_4 transport through sedges.

4.4 Functional genes during drought

Our results indicate that the abundance of functional genes related to CH_4 metabolism significantly change when exposed to drought conditions. 12% of the variance in abundances can be explained by year, with the highest variation in functional gene abundance observed under non-drought conditions. One possible explanation is that droughts increase the relative abundance of genera with greater genetic capacities to survive drought conditions, since these individuals can take better advantage of the aerobic conditions that inhibit metabolic activity in other genera.

The top three genes that contributed the most to the dissimilarity during the drought were *hdrA,* carbon monoxide dehydrogenase large subunit (*cutL*) and hydrogen dehydrogenase. The *hdrA,* combined with methyl-coenzyme M (*mcrA*), function together in the biological formation of CH_4. *mcrA* catalyzes the conversion of methyl-coenzyme M and coenzyme B into CH_4 and the heterodisulfide of coenzyme M (HS-CoM) and coenzyme B (HS-CoB) (Scheller et al., 2010, Thauer, 2019). Subsequently, CoM and CoB must be reduced to regenerate the CoM-SH and CoB-SH thiols that are used as electron donors by *mcrA,* which is then catalyzed by *hdrA* (Scheller et al., 2010, Buan et al., 2011). White et al. (2022) observed a co-dependence between *mcrA* and *hdrA,* indicating the close nature of the two genes for the biological formation of CH_4. Here we observe significant increases in the relative abundance of *hdrA* – but not *mcrA* –potentially resulting in a reduction in the conversion of *mcrA* and coenzyme B into CH_4. The lower fluxes suggest this, but it is challenging to determine whether the abundances of *hdrA* come exclusively from methanogens, as *hdrA* is a common gene shared between multiple microbial groups including *Acetogens,* sulfur oxidizing *Archaea* and *Bacteria* (Ernst et al., 2021). Therefore, it is difficult to determine whether the increase is related to methanogens or other microbial communities. In addition, we observed significant increases in the relative abundance of carbon monoxide dehydrogenase genes (*cutL*, *coxL*, *coxS* and *cutM*) under drought conditions. According to Ferry (2010), it is not yet known if carbon monoxide is a viable energy source for methanogens in peatland environments. The association between methanogenesis and the Acetyl-CoA pathway appears to be much more flexible than previously thought (Borrel et al., 2016).

4.5 Taxonomic diversity

In 2017, the mean α-diversity was 2.30 (± 0.24), while in 2018 the mean α-diversity was 2.49 (±0.25), but this is a non-significant difference. Between ecotypes, diversity was determined with the β-diversity index (Figure 7). During 2017, the highest mean distance of group members to the group centroid was observed in *R. alba* plots (0.36 ± 0.26) followed by *E. vaginatum* (0.33 ± 0.11) and *C. vulgaris* (0.33 ± 0.13). In 2018, this order was not observed and the *C. vulgaris* ecotype had the highest mean β-diversity (0.36 ± 0.0), followed by *R. alba (0.25* ± 0.09) and *E. vaginatum* (0.17 ± 0.09). Although we see small shifts between ecotypes and years, the ANOVA's p-value is not significant, meaning that group dispersions are homogenous ($p \geq 0.05$).

5 Conclusions

Our study provides in-situ evidence on how drought affects the functional potential of microorganisms responsible for CH_4 production and oxidation in hemi-boreal peatlands. The functional potential during the drought differed significantly when compared to the previous year. In response to the drought, the proportion of methanogens to methanotrophs shifted in favor of methanotrophs, driven by the facultative *Methylocella*. Our results suggest that (I) specific functional groups respond differently to drought events due advantageous genomic traits giving a competitive edge when under oxidative stress, (II) the diversity of methanogens and methanotrophs does not change under drought and that not one type of ecotype holds the best ecological niche, and finally, (III) peatlands dominated by sedge species *E. vaginatum* yield the highest fluxes of CH_4 under drought conditions. To be able to predict the effect of anthropogenic climate change, including drought events more accurately on methanogen and methanotroph communities, additional attention should be paid towards the frequency and length of drought events. We observe a highly resilient methanogen community, which surprisingly expanded in relative abundance during drought conditions, but this increase is not reflected in CH_4 emissions presumably due to the even higher increase in methanotrophy. This high abundance of both communities indicates that the severe drought from 2018 did not deteriorate the functional potential of the peatland ecosystem to emit CH_4 to the atmosphere.

Acknowledgments

We would like to thank the staff from the Centre for Genomic Research, Liverpool and Roche Diagnostics Scandinavia for probe hybridization and sequencing. Special thanks go to our colleagues, friends and family for the valuable discussions, and a special thank you to field assistants Oskar Ström and Thomas Golin for working hard during 2018 the heatwave. This study has been made possible by the Swedish Infrastructure for Ecosystem Science (SITES), at the Skogaryd research catchment station. SITES receives funding through the Swedish Research Council under the grant no 2019/8-365 and 2017-00635. Data handling was enabled by resources in project SNIC 2019/8-365 provided by the Swedish National Infrastructure for Computing (SNIC) at UPPMAX.

Open Research

The annotated seq
uence data used for analysing the functional potential of the microbial community in the study are available at the MG-RAST repository via project ID: 91145 with open access to public. The supplement related to the article is available online at https://zenodo.org/record/7472945#.Y6RT9xXMJaQ.

References

Amodeo, C., Sofo, A., Tito, M. T., Scopa, A., Masi, S., Pascale, R., . . . Caniani, D. (2018). Environmental factors influencing landfill gas biofiltration: Lab scale study on methanotrophic bacteria growth. *J Environ Sci Health A Tox Hazard Subst Environ Eng, 53*(9), 825-831. doi:10.1080/10934529.2018.1455342

Anderson, M. J. (2001). A new method for non-parametric multivariate analysis of variance. *Austral Ecology, 26*(1), 32-46. doi:10.1046/j.1442-9993.2001.01070.x

Angel, R., Matthies, D., & Conrad, R. (2011). Activation of Methanogenesis in Arid Biological Soil Crusts Despite the Presence of Oxygen. *PLOS ONE, 6*(5), 1-8. doi:10.1371/journal.pone.0020453

Bates, D., Mächler, M., Bolker, B., & Walker, S. (2015). Fitting Linear Mixed-Effects Models Using lme4. *Journal of Statistical Software, 67*(1), 1 - 48. doi:10.18637/jss.v067.i01

Borrel, G., Adam, P. S., & Gribaldo, S. (2016). Methanogenesis and the Wood-Ljungdahl Pathway: An Ancient, Versatile, and Fragile Association. *Genome Biol Evol, 8*(6), 1706-1711. doi:10.1093/gbe/evw114

Brandt, F. B., Martinson, G. O., Pommerenke, B., Pump, J., & Conrad, R. (2015). Drying effects on archaeal community composition and methanogenesis in bromeliad tanks. *FEMS Microbiology Ecology, 91*(2). doi:10.1093/femsec/iu021

Bräuer, S. L., Basiliko, N., M. P. Siljanen, H., & H. Zinder, S. (2020). Methanogenic archaea in peatlands. *FEMS Microbiology Letters, 367*(20). doi:10.1093/femsle/fnaa172

Buan, N., Kulkarni, G., & Metcalf, W. (2011). Chapter two - Genetic Methods for Methanosarcina Species. In A. C. Rosenzweig & S. W. Ragsdale (Eds.), *Methods in Enzymology* (Vol. 494, pp. 23-42): Academic Press.

Conrad, R., Ji, Y., Noll, M., Klose, M., Claus, P., & Enrich-Prast, A. (2014). Response of the methanogenic microbial communities in Amazonian oxbow lake sediments to desiccation stress. *Environmental microbiology, 16*(6), 1682-1694. doi:10.1111/1462-2920.12267

Dean, J. F., Middelburg, J. J., Röckmann, T., Aerts, R., Blauw, L. G., Egger, M., . . . Dolman, A. J. (2018). Methane Feedbacks to the Global Climate System in a Warmer World. *Reviews of Geophysics, 56*(1), 207-250. doi:doi:10.1002/2017RG000559

Dedysh, S. N., & Dunfield, P. F. (2011). Chapter three - Facultative and Obligate Methanotrophs: How to Identify and Differentiate Them. In A. C. Rosenzweig & S. W. Ragsdale (Eds.), *Methods in Enzymology* (Vol. 495, pp. 31-44): Academic Press.

Erkel, C., Kube, M., Reinhardt, R., & Liesack, W. (2006). Genome of Rice Cluster I Archaea: The Key Methane Producers in the Rice Rhizosphere. *Science, 313*(5785), 370-372.

Ernst, C., Kayastha, K., Koch, T., Venceslau, S. S., Pereira, I. A. C., Demmer, U., . . . Dahl, C. (2021). Structural and spectroscopic characterization of a HdrA-like subunit from Hyphomicrobium denitrificans. *The FEBS Journal, 288*(5), 1664-1678. doi:https://doi.org/10.1111/febs.15505

Fenner, N., & Freeman, C. (2011). Drought-induced carbon loss in peatlands. *Nature Geoscience, 4*(12), 895-900. doi:10.1038/ngeo1323

Ferry, J. G. (1999). Enzymology of one-carbon metabolism in methanogenic pathways. *FEMS Microbiology Reviews, 23*(1), 13-38. doi:doi:10.1111/j.1574-6976.1999.tb00390.x

Ferry, J. G. (2010). CO in methanogenesis. *Annals of Microbiology, 60*(1), 1-12. doi:10.1007/s13213-009-0008-5

Hakobyan, A., & Liesack, W. (2020). Unexpected metabolic versatility among type II methanotrophs in the Alphaproteobacteria. *Biological Chemistry, 401*(12), 1469-1477. doi:doi:10.1515/hsz-2020-0200

Ho, A., Lüke, C., & Frenzel, P. (2011). Recovery of methanotrophs from disturbance: population dynamics, evenness and functioning. *The ISME journal, 5*(4), 750-758. doi:10.1038/ismej.2010.163

Ho, A., van den Brink, E., Reim, A., Krause, S. M., & Bodelier, P. L. (2015). Recurrence and Frequency of Disturbance have Cumulative Effect on Methanotrophic Activity, Abundance, and Community Structure. *Front Microbiol, 6*, 1493. doi:10.3389/fmicb.2015.01493

IPCC. (2021). Climate Change 2021: The Physical Science Basis. Contribution of Working Group I to the Sixth Assessment Report of the Intergovernmental Panel on Climate Change Masson-Delmotte, V., P. Zhai, A. Pirani, S.L. Connors, C. Péan, S. Berger, N. Caud, Y. Chen, L. Goldfarb, M.I. Gomis, M. Huang, K. Leitzell, E. Lonnoy, J.B.R. Matthews, T.K. Maycock, T. Waterfield, O. Yelekçi, R. Yu, and B. Zhou (eds.). *Cambridge University Press*.

Joshi, N. (2011). Sickle: A sliding-window, adaptive, quality-based trimming tool for FastQ files (Version 1.33). Retrieved from https://github.com/najoshi/sickle

Kanehisa, M., Sato, Y., Kawashima, M., Furumichi, M., & Tanabe, M. (2015). KEGG as a reference resource for gene and protein annotation. *Nucleic Acids Research, 44*(D1), D457-D462. doi:10.1093/nar/gkv1070

Keane, B. J., Ineson, P., Vallack, H. W., Blei, E., Bentley, M., Howarth, S., . . . Toet, S. (2018). Greenhouse gas emissions from the energy crop oilseed rape (Brassica napus); the role of photosynthetically active radiation in diurnal N2O flux variation. *GCB Bioenergy, 10*(5), 306-319. doi:https://doi.org/10.1111/gcbb.12491

Keane, J. B., Toet, S., Ineson, P., Weslien, P., Stockdale, J. E., & Klemedtsson, L. (2021). Carbon Dioxide and Methane Flux Response and Recovery From Drought in a Hemiboreal Ombrotrophic Fen. *Frontiers in Earth Science, 8*(706). doi:10.3389/feart.2020.562401

Kelly, J., Kljun, N., Eklundh, L., Klemedtsson, L., Liljebladh, B., Olsson, P.-O., . . . Xie, X. (2021). Modelling and upscaling ecosystem respiration using thermal cameras and

UAVs: Application to a peatland during and after a hot drought. *Agricultural and Forest Meteorology, 300*, 108330. doi:https://doi.org/10.1016/j.agrformet.2021.108330

Kim, B.-R., Shin, J., Guevarra, R., Lee, J. H., Kim, D. W., Seol, K.-H., . . . Isaacson, R. (2017). Deciphering Diversity Indices for a Better Understanding of Microbial Communities. *Journal of microbiology and biotechnology, 27*(12), 2089-2093. doi:10.4014/jmb.1709.09027

Kim, S.-Y., Lee, S.-H., Freeman, C., Fenner, N., & Kang, H. (2008). Comparative analysis of soil microbial communities and their responses to the short-term drought in bog, fen, and riparian wetlands. *Soil Biology and Biochemistry, 40*(11), 2874-2880. doi:https://doi.org/10.1016/j.soilbio.2008.08.004

Kip, N., van Winden, J. F., Pan, Y., Bodrossy, L., Reichart, G.-J., Smolders, A. J. P., . . . Op den Camp, H. J. M. (2010). Global prevalence of methane oxidation by symbiotic bacteria in peat-moss ecosystems. *Nature Geoscience, 3*(9), 617-621. doi:10.1038/ngeo939

Korrensalo, A., Männistö, E., Alekseychik, P., Mammarella, I., Rinne, J., Vesala, T., & Tuittila, E. S. (2018). Small spatial variability in methane emission measured from a wet patterned boreal bog. *Biogeosciences, 15*(6), 1749-1761. doi:10.5194/bg-15-1749-2018

Kushwaha, S. K., Manoharan, L., Meerupati, T., Hedlund, K., & Ahren, D. (2015). MetCap: a bioinformatics probe design pipeline for large-scale targeted metagenomics. *BMC Bioinformatics, 16*, 65. doi:10.1186/s12859-015-0501-8

Liebner, S., Zeyer, J., Wagner, D., Schubert, C., Pfeiffer, E.-M., & Knoblauch, C. (2011). Methane oxidation associated with submerged brown mosses reduces methane emissions from Siberian polygonal tundra. *Journal of Ecology, 99*(4), 914-922. doi:https://doi.org/10.1111/j.1365-2745.2011.01823.x

Lyu, Z., & Lu, Y. (2018). Metabolic shift at the class level sheds light on adaptation of methanogens to oxidative environments. *The ISME journal, 12*(2), 411-423. doi:10.1038/ismej.2017.173

Ma, K., Conrad, R., & Lu, Y. (2012). Responses of methanogen mcrA genes and their transcripts to an alternate dry/wet cycle of paddy field soil. *Applied and Environmental Microbiology, 78*(2), 445-454. doi:10.1128/AEM.06934-11

Manoharan, L., Kushwaha, S. K., Hedlund, K., & Ahren, D. (2015). Captured metagenomics: large-scale targeting of genes based on 'sequence capture' reveals functional diversity in soils. *DNA Res, 22*(6), 451-460. doi:10.1093/dnares/dsv026

Martin, M. (2011). Cutadapt removes adapter sequences from high-throughput sequencing reads. *2011, 17*(1), 3. doi:10.14806/ej.17.1.200

McMurdie, P. J., & Holmes, S. (2013). phyloseq: An R Package for Reproducible Interactive Analysis and Graphics of Microbiome Census Data. *PLOS ONE, 8*(4), e61217. doi:10.1371/journal.pone.0061217

Meyer, F., Paarmann, D., D'Souza, M., Olson, R., Glass, E. M., Kubal, M., . . . Edwards, R. A. (2008). The metagenomics RAST server – a public resource for the automatic phylogenetic and functional analysis of metagenomes. *BMC Bioinformatics, 9*(1), 386. doi:10.1186/1471-2105-9-386

Miller, K. E., Lai, C.-T., Dahlgren, R. A., & Lipson, D. A. (2019). Anaerobic Methane Oxidation in High-Arctic Alaskan Peatlands as a Significant Control on Net CH4 Fluxes. *Soil Systems, 3*(1), 7.

O'Leary, N. A., Wright, M. W., Brister, J. R., Ciufo, S., Haddad, D., McVeigh, R., . . . Pruitt, K. D. (2016). Reference sequence (RefSeq) database at NCBI: current status, taxonomic expansion, and functional annotation. *Nucleic Acids Res, 44*(D1), D733-745. doi:10.1093/nar/gkv1189

Oksanen, J., Blanchet, F. G., Friendly, M., Kindt, R., Legendre, P., McGlinn, D., . . . Wagner, H. (2019). vegan: Community Ecology Package.

R Core Team. (2018). R: A language and environment for statistical computing. Viena, Austria: R-Foundation for Statistical Computing. Retrieved from https://www.R-project.org/

Rinne, J., Tuovinen, J.-P., Klemedtsson, L., Aurela, M., Holst, J., Lohila, A., . . . Nilsson, M. B. (2020). Effect of the 2018 European drought on methane and carbon dioxide exchange of northern mire ecosystems. *Philosophical Transactions of the Royal Society B: Biological Sciences, 375*(1810), 20190517. doi:doi:10.1098/rstb.2019.0517

Saunois, M., Stavert, A. R., Poulter, B., Bousquet, P., Canadell, J. G., Jackson, R. B., . . . Zhuang, Q. (2020). The Global Methane Budget 2000–2017. *Earth Syst. Sci. Data, 12*(3), 1561-1623. doi:10.5194/essd-12-1561-2020

Scheller, S., Goenrich, M., Boecher, R., Thauer, R. K., & Jaun, B. (2010). The key nickel enzyme of methanogenesis catalyses the anaerobic oxidation of methane. *Nature, 465*(7298), 606-608. doi:10.1038/nature09015

Sjökvist, E., Abdoush, D., & Axén, J. (2019). Sommaren 2018 - en glimt av framtiden? SMHI. *Klimatologi, 52*.

Thauer, R. K. (2019). Methyl (Alkyl)-Coenzyme M Reductases: Nickel F-430-Containing Enzymes Involved in Anaerobic Methane Formation and in Anaerobic Oxidation of Methane or of Short Chain Alkanes. *Biochemistry, 58*(52), 5198-5220. doi:10.1021/acs.biochem.9b00164

Thauer, R. K., Kaster, A.-K., Seedorf, H., Buckel, W., & Hedderich, R. (2008). Methanogenic archaea: ecologically relevant differences in energy conservation. *Nature Reviews Microbiology, 6*(8), 579-591. doi:10.1038/nrmicro1931

van Hulzen, J. B., Segers, R., van Bodegom, P. M., & Leffelaar, P. A. (1999). Temperature effects on soil methane production: an explanation for observed variability. *Soil Biology and Biochemistry, 31*(14), 1919-1929. doi:https://doi.org/10.1016/S0038-0717(99)00109-1

Vicente-Serrano, S. M., Beguería, S., & López-Moreno, J. I. (2010). A Multiscalar Drought Index Sensitive to Global Warming: The Standardized Precipitation Evapotranspiration Index. *Journal of Climate, 23*(7), 1696-1718. doi:10.1175/2009jcli2909.1

Villanueva, R. A. M., & Chen, Z. J. (2019). ggplot2: Elegant Graphics for Data Analysis (2nd ed.). *Measurement: Interdisciplinary Research and Perspectives, 17*(3), 160-167. doi:10.1080/15366367.2019.1565254

Wallin, M. B., Weyhenmeyer, G. A., Bastviken, D., Chmiel, H. E., Peter, S., Sobek, S., & Klemedtsson, L. (2015). Temporal control on concentration, character, and export of dissolved organic carbon in two hemiboreal headwater streams draining contrasting catchments. *Journal of Geophysical Research: Biogeosciences, 120*(5), 832-846. doi:https://doi.org/10.1002/2014JG002814

Wendlandt, K.-D., Stottmeister, U., Helm, J., Soltmann, B., Jechorek, M., & Beck, M. (2010). The potential of methane-oxidizing bacteria for applications in environmental biotechnology. *Engineering in Life Sciences, 10*(2), 87-102. doi:https://doi.org/10.1002/elsc.200900093

White, J. D., Ström, L., Lehsten, V., Rinne, J., & Ahrén, D. (2022). Genetic functional potential displays minor importance in explaining spatial variability of methane fluxes within a Eriophorum vaginatum dominated Swedish peatland. *Biogeosciences Discuss., 2022*, 1-38. doi:10.5194/bg-2021-353

Wilmoth, J. L., Schaefer, J. K., Schlesinger, D. R., Roth, S. W., Hatcher, P. G., Shoemaker, J. K., & Zhang, X. (2021). The role of oxygen in stimulating methane production in wetlands. *Global Change Biology, 27*(22), 5831-5847. doi:https://doi.org/10.1111/gcb.15831

Yu, Z. C. (2012). Northern peatland carbon stocks and dynamics: a review. *Biogeosciences, 9*(10), 4071-4085. doi:10.5194/bg-9-4071-2012

Yuan, Y., Conrad, R., & Lu, Y. (2009). Responses of methanogenic archaeal community to oxygen exposure in rice field soil. *Environ Microbiol Rep, 1*(5), 347-354. doi:10.1111/j.1758-2229.2009.00036.x

Zhong, Q., Chen, H., Liu, L., He, Y., Zhu, D., Jiang, L., . . . Hu, J. (2017). Water table drawdown shapes the depth-dependent variations in prokaryotic diversity and structure in Zoige peatlands. *FEMS Microbiology Ecology, 93*(6). doi:10.1093/femsec/fix049

Figure 1: (a) Location of Mycklemossen (black star) within Sweden (b) aerial photo of Mycklemossen, black square shows the location of the sampling area and (c), map of peat core and ancillary measurement locations. Map data sources: © EuroGeographics and © Lantmäteriet.

Figure 2: A) Daily mean temperature measured in °C and B) Daily summed precipitation measured in millimeters at Mycklemossen mire. 2017 is shown in blue and 2018 in red. The shaded area indicates the growing season from May 1st to September 30th.

Figure 3: Daily mean soil temperature measured at 6 cm and 30 cm below the peat surface. Blue lines indicate 2017 values while red lines indicate 2018 values. The shaded area indicates the growing season from May 1st to September 30th.

Figure 4: Water table depth in meters below the surface for *C. vulgaris*, *E. vaginatum* and *R. alba* ecotypes from automated sensors at the site during 2017 (A) and 2018 (B). The shaded area indicates the growing season from May 1st and September 30th.

Figure 5: Boxplots of daily mean CH_4 flux measured during the growing season (May to October) in 2017 (blue) and 2018 (red) at Mycklemossen mire. The boxes show quartiles and the median, the whiskers denote data within 1.5 times of the interquartile range. Colored stars denote outliers while significant differences using linear mixed effects models are labelled with the p value and "n.s." indicates a non-significant result.

Figure 6: Non-metric Multidimensional Scaling (NMDS) of taxonomic abundances using Bray-Curtis distances. Small dots indicate individual samples while the largest dots indicate the mean of all samples. Samples were analyzed at genus level and colored by year 2017 (n = 17) and 2018 (n = 10).

Figure 7: Principal Coordinates Analysis (PCoA) of taxonomic abundances using Bray-Curtis distances. Small symbols indicate individual samples while the largest symbols indicate the mean of all samples. Samples were analyzed at genus level and colored by ecotype and sampling year (*C. vulgaris* 2017 (n = 6) 2018 (n = 2), *E. vaginatum* 2017 (n = 7) 2018 (n = 4), *R. alba* 2017 (n = 4) 2018 (n = 4).

Figure 8: Nonmetric Multidimensional Scaling (NMDS) of functional genes using Bray-Curtis distances. Small dots indicate individual samples while the largest dots indicate the mean of all samples. Samples were analyzed at KO level 4 and colored by year 2017 (n = 17) and 2018 (n = 10).

Table 1: Results of taxonomic contribution of each species (%) to the dissimilarity between each group (SIMPER analysis) between 2017 and 2018. Taxa are ranked according to their average contribution to dissimilarity between years. Average abundances, percentage of cumulative contribution and Permutation *p*-value (Probability of getting a larger or equal average contribution in random permutation of the group factor) are also included. A cut-off at a cumulative dissimilarity of 70% was applied (2017 n = 17: 2018 n = 10).